Prethermal Fragmentation in a Periodically Driven Fermionic Chain

Somsubhra Ghosh,[1] Indranil Paul,[2] and K. Sengupta[1]
[1]School of Physical Sciences, Indian Association for the Cultivation of Science, Kolkata 700032, India
[2]Université Paris Cité, CNRS, Laboratoire Matériaux et Phénomènes Quantiques, 75205 Paris, France

(Received 14 December 2022; revised 9 February 2023; accepted 3 March 2023; published 23 March 2023)

We study a fermionic chain with nearest-neighbor hopping and density-density interactions, where the nearest-neighbor interaction term is driven periodically. We show that such a driven chain exhibits prethermal strong Hilbert space fragmentation (HSF) in the high drive amplitude regime at specific drive frequencies ω_m^*. This constitutes the first realization of HSF for out-of-equilibrium systems. We obtain analytic expressions of ω_m^* using a Floquet perturbation theory and provide exact numerical computation of entanglement entropy, equal-time correlation functions, and the density autocorrelation of fermions for finite chains. All of these quantities indicate clear signatures of strong HSF. We study the fate of the HSF as one tunes away from ω_m^* and discuss the extent of the prethermal regime as a function of the drive amplitude.

DOI: 10.1103/PhysRevLett.130.120401

Eigenstate thermalization hypothesis (ETH) conjectures that midspectrum eigenstates of an isolated quantum system are locally thermal [1–4]. A similar thermal characteristic leading to an infinite temperature steady state is seen for periodically driven systems [5,6]. In both cases, ETH has been immensely successful in predicting the longtime dynamical behavior of local operators of isolated quantum systems. However, for periodically driven systems experimentally relevant timescales may be significantly shorter than their thermalization times [7–9]. It is well known that the resultant prethermal phases may exhibit interesting phenomena that have no equilibrium analog [9–18].

The violation of ETH due to lack of ergodicity can occur in integrable quantum systems [3,4] or in systems with strong disorder in their many body localized phases [8,19,20]. A weaker violation of ETH can also occur for Hamiltonians hosting quantum scars [21–25]. The presence of such scars in eigenstates of a Floquet Hamiltonian has also been studied [17,18,26–28].

ETH violation can also occur from fragmentation of Hilbert space of a quantum system due to the presence of kinetic constraints [29–38]. The Hamiltonian of such systems, in the computational basis, breaks down into several dynamically disconnected blocks. For strong Hilbert space fragmentation (HSF), the number of such blocks increases exponentially with the system size [29–38]; this is distinct from algebraic scaling of the number of disconnected symmetry sectors. All the studies of strong HSF, so far, have involved equilibrium Hamiltonians; to the best of our knowledge, there has been no example of the existence of strong HSF in out-of-equilibrium quantum systems. In this Letter we provide the first example of prethermal HSF in a periodically driven Fermi chain with large drive amplitude at special drive frequencies.

To this end, we consider a fermion chain with a Hamiltonian given by $H(t) = H_0(t) + H_1$

$$H_0(t) = V(t) \sum_{j=1..L} \hat{n}_j \hat{n}_{j+1}$$
$$H_1 = \sum_{j=1..L} -J(c_j^\dagger c_{j+1} + \text{H.c.}) + \hat{n}_j(V_0 \hat{n}_{j+1} + V_2 \hat{n}_{j+2}), \tag{1}$$

where c_j denotes the fermion annihilation operator for the site j of the chain, $\hat{n}_j = c_j^\dagger c_j$ is the fermion density operator, $V_0 + V(t)$ and V_2 are the strengths of nearest- and next-nearest neighbor interactions, respectively. In what follows, we drive this chain by making $V(t)$ periodic in time with an amplitude $V_1 \gg V_0, J, V_2$ and frequency $\omega_D = 2\pi/T$, where T is the drive time period. The precise form of $V(t)$ depends on the drive protocol; in this Letter we shall study both continuous cosine [$V(t) = V_1 \cos \omega_D t$] and discrete square-pulse [$V(t) = -(+)V_1$ for $t \leq (>)T/2$] protocols.

Our results are as follows. First, we derive the Floquet Hamiltonian of the driven chain in the high amplitude limit using Floquet perturbation theory (FPT). We show that at special drive frequencies $\omega_D = \omega_m^*$, whose analytic expression we provide, the first order Floquet Hamiltonian, $H_F^{(1)}$, of the system reduces to a fermionic model with constrained hopping which is known to exhibit HSF [32,33]. In the high-drive amplitude regime, the higher order correction to $H_F^{(1)}$ are small; consequently, the driven system exhibits signatures of fragmentation over a long prethermal regime. Second, we supplement the analytical result by numerical computation of the exact time evolution operator

$U(T,0)$ using exact diagonalization (ED) on Eq. (1). We obtain exact evolution of the half-chain von Neumann entanglement entropy $S(nT)$, starting from a random Fock state, as a function of the number of drive cycles n. We find that away from ω_m^*, $S(nT)$ reaches the symmetry resolved Page value S_p, as expected for nonintegrable ergodic driven systems [39]; in contrast, at $\omega_D = \omega_m^*$ and for large V_1, $S(nT)$ saturates to the Page value S_p^f of the Hilbert space fragment of $H_F^{(1)}$ to which the initial state belongs for a long range of n. Third, using ED, we compute the exact fermion density autocorrelation function

$$C_j(nT) = \langle\psi_0|[\hat{n}_j(nT) - 1/2][\hat{n}_j(0) - 1/2]|\psi_0\rangle \quad (2)$$

starting from a random infinite-temperature initial state $|\psi_0\rangle$. We find that $C_j(nT)$ does not attain its ETH predicted value at $\omega_D = \omega_m^*$ beyond a critical V_1; instead, it saturates to a finite value, larger than a lower bound that can be obtained using Mazur's inequality [30,31,40,41], as expected in a system with strong HSF [29]. In contrast, for $\omega_D \neq \omega_m^*$, C_j obeys ETH. Fourth, we study the equal-time correlation function

$$\chi_j(nT) = \langle\psi_f(nT)|\hat{n}_j\hat{n}_{j+2}|\psi_f(nT)\rangle \quad (3)$$

of fermions starting from frozen states (Fock states $|\psi_f\rangle$ which are eigenstates of $H_F^{(1)}$). The dynamics of these states, at $\omega_D = \omega_m^*$, arise solely due to the presence of higher order terms in the Floquet Hamiltonian which is well captured in our exact numerics obtained using ED on $H(t)$ [Eq. (1)]. We find that for large V_1, $\chi(nT)$ remain close to their initial values at $\omega_D = \omega_m^*$ over a large range of n for random frozen initial states. In contrast, they saturate to the ETH predicted value at other frequencies. Moreover, for the frozen state $|\psi_f\rangle = |\mathbb{Z}_2\rangle \equiv |0,1,0,1,\ldots\rangle$, we find the existence of novel oscillatory dynamics of $\chi_j(nT)$ when $J/V_0 \ll 1$; we provide a semianalytic explanation of this dynamics and tie the existence of such oscillations to both the broken Z_2 symmetry of the initial Fock state and the presence of HSF which confines the dynamics to a small class of states in the Hilbert space.

FPT and Floquet Hamiltonian.—To derive the Floquet Hamiltonian for the driven chain, we start from Eq. (1) and adapt a perturbative scheme (FPT), where J/V_1 is the small parameter; this distinguishes it from standard high-frequency Magnus expansion [42–44]. Within this scheme, one computes the evolution operator corresponding to $H_0(t)$ exactly; $U_0(t,0) = \mathcal{T}\exp[-i\int_0^t dt' H_0(t')/\hbar]$, where $\mathcal{T}$ is the time ordering operator. The contribution of H_1 to the full evolution operator $U(t,0)$ is then computed using standard perturbation theory. To first order in perturbation, this leads to $U_1(T,0) = (-i/\hbar)\int_0^T dt[U_0(t,0)]^\dagger H_1 U_0(t,0)$ and yields the leading order Floquet Hamiltonian $H_F^{(1)} = i\hbar U_1(T,0)/T$. A straightforward calculation detailed in [41] leads to

$$H_F^{(1)} = \sum_{j=1..L} \hat{n}_j(V_0\hat{n}_{j+1} + V_2\hat{n}_{j+2}) - J\sum_{j=1..L}[(1-\hat{A}_j^2) + f(\gamma_0)\hat{A}_j^2]c_j^\dagger c_{j+1} + \text{H.c.}, \quad (4)$$

where $\hat{A}_j = (\hat{n}_{j+2} - \hat{n}_{j-1})$, $\gamma_0 = V_1 T/(4\hbar)$, and $f(\gamma_0) = J_0[2\gamma_0/\pi]$ for the cosine protocol and $f(\gamma_0) = \gamma_0^{-1}\sin\gamma_0\exp[i\gamma_0\hat{A}_j]$ for the square-pulse protocol, where J_0 is the zeroth order Bessel function.

Equation (4) represents one of the central results of this Letter; it shows the existence of special drive frequencies $\omega_D = \omega_m^*$ for which $f(\gamma_0) = 0$. These correspond to $\gamma_0 = \pi\zeta_m/2$ and $\gamma_0 = m\pi$, respectively, for the cosine and square-pulse protocols, where m is a positive integer and ζ_m denotes the position of the mth zero of J_0. This yields

$$\omega_m^* = V_1/(\hbar\zeta_m) \quad \text{for cosine protocol}$$
$$= V_1/(2\hbar m) \quad \text{for square-pulse protocol.} \quad (5)$$

At these frequencies, $H_F^{(1)}$ reduces to the constrained hopping Hamiltonian studied in Refs. [32,33] which is known to show strong HSF. Such constrained Hamiltonian hosts several conserved quantities, namely, the fermion density $N = \sum_j \hat{n}_j/L$, $N_d = \sum_j \hat{n}_j\hat{n}_{j+1}$, and $N_d' = \sum_j(-1)^j\hat{n}_j\hat{n}_{j+1}$; the corresponding Hilbert space splits into exponentially large number of fragments including exponentially large number of frozen states $|\psi_f\rangle$ [32,33]. Furthermore, in the high-drive amplitude regime, a straightforward calculation detailed in [41] shows that the higher order terms of H_F are suppressed by at least a factor of J/V_1. Thus in this regime, we expect the driven fermion chain to show signatures of HSF in the prethermal regime at $\omega_D = \omega_m^*$. For the rest of this Letter, we present our numerical results using the square-pulse protocol; the corresponding results for the cosine drive protocol is presented in Ref. [41].

Entanglement entropy.—To find the signature of fragmentation in the driven chain, we first study $S(nT)$ starting from a random Fock state $|\psi_0\rangle$ as a function of the number of drive cycles n. We numerically compute $U(T,0)$ using ED starting from $H(t)$ [Eq. (1)] as outlined in Ref. [41]. This allows us to obtain $|\psi(nT)\rangle = U(nT,0)|\psi_0\rangle$. One then constructs the density matrix $\rho(nT) = |\psi(nT)\rangle\langle\psi(nT)|$ for the driven chain. Finally, one carries out a partial trace of $\rho(nT)$ over half the chain, to obtain the reduced density matrix $\rho_{\text{red}}(nT)$ [17]; this leads to $S(nT) = -\text{Tr}[\rho_{\text{red}}(nT)\ln\rho_{\text{red}}(nT)]$.

For an ergodic chain, one expects $S(nT)$ to saturate to the symmetry resolved Page value S_p [39] corresponding to the symmetry sector to which the initial state belongs.

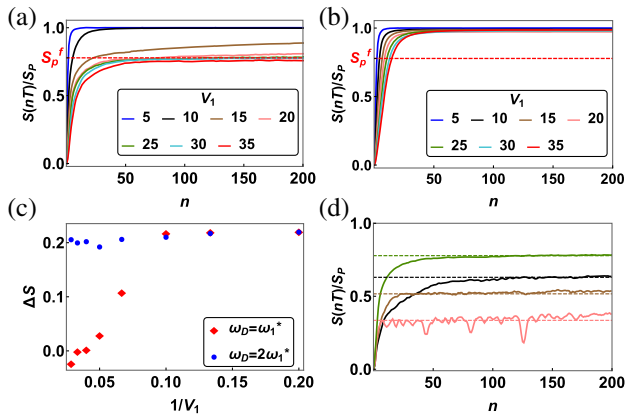

FIG. 1. (a) Plot of $S(nT)/S_p$ as a function of n for ω_1^* and several V_1 starting from a random Fock state. The red dotted line corresponds to S_p^f/S_p of the largest fragment of $H_F^{(1)}$ with HSD 1008 to which the initial state belongs. $S(nT)$ saturates to $S_p^f = 0.8S_p$ for large V_1 and $n \leq 200$. (b) Same as (a) but at $2\omega_1^*$; here S saturates to S_p for all V_1. (c) Plot of $\Delta S = (S(nT) - S_p^f)/S_p$ as a function of $1/V_1$ for $n = 200$. $\Delta S \to 0$ at ω_1^* and for large V_1. (d) Plot of $S(nT)/S_p$ for $V_1 = 25$ and at ω_1^* corresponding to several initial Fock states belonging to fragments of $H_F^{(1)}$ with HSD 1008 (green), 288 (black), 144 (brown), and 56 (pink). The dotted lines correspond to S_p^f/S_p to which $S(nT)/S_p$ saturates for $n \leq 200$. All plots indicate clear signature of prethermal strong HSF at ω_1^*. For all plots $L = 16$, $V_0 = V_2 = 2$ and all energies are scaled in units of J.

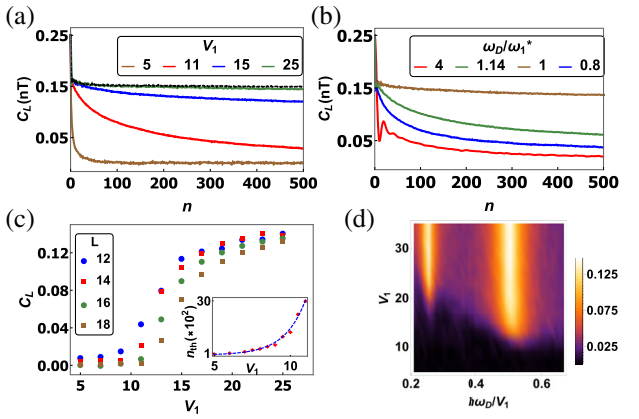

FIG. 2. (a) $C_L(nT)$ as a function of n at ω_1^* computed using exact H_F for several V_1 starting from a random thermal state. For large V_1, $C_L(nT)$ saturates to the black dotted line which corresponds to its value computed using $H_F^{(1)}$ indicating prethermal HSF. (b) Plot of $C_L(nT)$ as a function of n for several ω_D for $V_1 = 19$ showing ETH predicted thermalization away from ω_1^*. (c) Plot of $C_L(nT)$ for $n = 5000$ as a function of V_1 at ω_1^* for several L showing a clear crossover to a prethermal HSF regime at large V_1. The inset shows the number of cycles n_{th} required for $C_L(nT)$ to reach its ETH predicted value at ω_1^* for $L = 16$; n_{th} scales exponentially with V_1 showing a long prethermal regime at large V_1. (d) Phase diagram obtained from plot of $C_L(nT)$ for $n = 5000$ as a function of V_1 and $\hbar\omega_D/V_1$ showing clear signature of finite value of C_L at large V_1 at $\hbar\omega_{1(2)}^* = V_1/2(4)$. For all plots $V_0 = V_2 = 2$ and all energies are scaled in units of J. $L = 16$ for (a) and (b) and $L = 14$ for (d).

In contrast, for a system with HSF, it saturates to the Page value S_p^f of the fragment of $H_F^{(1)}$ to which the initial state belongs; since for strong HSF the Hilbert space dimension (HSD) of any fragment is exponentially smaller than the total HSD, $S_p^f < S_p$.

In Fig. 1, plots of $S(nT)$ corresponding to the symmetry sector $N = \sum_j n_j/L = 1/2$ are shown. For these plots we have chosen $V_0 = V_2 = 2J$ and used periodic boundary condition. Figure 1(a) shows that for $\omega_D = \omega_1^*$ and large V_1/J, $S(nT)$ saturates to $S_p^f \simeq 0.8S_p$ till $n \sim 200$. In contrast, it saturates to S_p for small V_1/J. We find a clear crossover between these two regimes. This behavior is to be contrasted with its counterpart at $2\omega_1^*$ [Fig. 1(b)], where $S(nT)$ always saturates to S_p within $n \leq 50$. The dependence of $\Delta S = [S(nT) - S_p^f]/S_p$ on $1/V_1$ for both ω_1^* (red dots) and $2\omega_1^*$ (blue dots) for $n = 200$ is shown in Fig. 1(c). The latter always stays finite indicating proximity to S_p while the former sharply drops to zero beyond a critical drive amplitude. Finally, we compute $S(nT)/S_p$ for several random Fock states which belong to different Hilbert space fragments of $H_F^{(1)}$. We find that for $V_1/J = 25$ and at ω_1^*, $S(nT)$ for these initial states saturate to their respective S_p^f. All these features show a clear signature of prethermal HSF at ω_1^*.

Autocorrelation.—For further signature of HSF at large V_1, we study the autocorrelation function $C_{j=L}(nT) \equiv C_L(nT)$ [Eq. (2)] using ED and starting from Eq. (1), as a function of n. We use open boundary condition and set $V_0 = V_2 = 2J$. It is well known that the presence of HSF leads to a finite long-term value of the autocorrelator which is bounded from below [30,31,40,41]; for the present system, this bound is estimated to be 0.125 [41]. In contrast it decays to its ETH predicted value, $C_{\text{ETH}} = 0$, in the absence of HSF. The behavior of $C_j(nT)$ for $j \neq L$ is qualitatively similar [31,41].

Figure 2(a) shows the behavior of $C_L(nT)$ as a function of n at ω_1^* for several V_1/J. We again find that for large V_1/J, $C_L(nT)$ stays above the lower bound 0.125 and close to its value predicted by $H_F^{(1)}$ exhibiting strong HSF for a large number of drive cycles. The behavior of $C_L(nT)$ for other drive frequencies is shown in Fig. 2(b) for $V_1 = 25J$; the plot clearly indicates that deviation from ω_1^* leads to rapid, ETH predicted, thermalization of $C_L(nT)$.

The plot of $C_L(nT)$ for $n = 5000$ at ω_1^* is shown as a function of V_1/J in Fig. 2(c) for several system sizes (L). We find C_L becomes almost independent of L at both large and small V_1/J; in between, the crossover region reduces in width with increasing L. This may indicate a sharp

transition in the thermodynamic limit; however, it is difficult to conclude this from the present data.

The inset of Fig. 2(c), shows a plot of $n_{\rm th}$, the number of drive cycles required for C_L to reach the ETH predicted value, as a function of V_1/J. The data clearly demonstrates exponential scaling of $n_{\rm th}$ with V_1/J [7,45,46]. A numerical fit suggests $n_{\rm th} \sim \exp[0.72V_1/J]$. This behavior of $n_{\rm th}$ can be understood as follows. It is expected that for large ω_D, the extent of the prethermal regime scales exponentially with ω_D: $n_{\rm th} \sim \exp[c_0\hbar\omega_D/J]$ where c_0 is a constant [45]. In the present case, $\omega_D = \omega_1^*$; so one expects $n_{\rm th} = \exp[c_0V_1/(2J)]$ which yields the exponential scaling. The numerical value of c_0 is determined to be order unity from our numerics; an analytic estimate of c_0, which necessitates information about breakdown of convergence of the FPT series, is beyond the scope of the present Letter. However, we would like to point out that this exponential scaling indicates a long and stable prethermal regime where HSF signatures can be found.

Finally, in Fig. 2(d), we show a phase diagram distinguishing between regimes displaying ETH predicted thermal and HSF features of C_L as a function of V_1/J and $\hbar\omega_D/V_1$. The plot represents a clear crossover between the two regimes at both $\omega_1^* = V_1/(2\hbar)$ and $\omega_2^* = V_1/(4\hbar)$ as V_1/J is increased; we note that this is consistent with our theoretical expectation based on $H_F^{(1)}$.

Dynamics of frozen states.—The frozen states correspond to Fock states which are eigenstates of $H_F^{(1)}$; however, they have nontrivial evolution under H_F due to higher order terms in FPT. The nature of this evolution, for a random frozen state with no particular symmetries, is expected to obey ETH away from ω_m^*; in contrast, at ω_m^*, they are expected to stay close to their initial values at large drive amplitudes for a wide range of n.

To capture this behavior we numerically compute $\chi_{j=1}(nT) \equiv \chi_1(nT)$ [Eq. (3)] using ED and starting from Eq. (1) and plot it as a function of n in Fig. 3(a) for ω_1^* and $6\omega_1^*$ at $V_1 = 19J$. These computations are done for chains with periodic boundary conditions and $V_0 = 10V_2 = 2J$. The plot clearly shows that $\chi_1(nT)$ reaches its ETH predicted value for $6\omega_1^*$; in contrast it never reaches the ETH predicted value at ω_1^*. The plot of $\langle\chi_1\rangle$ [$\chi_1(nT)$ averaged over 5000 drive cycles starting from $n = 5000$] as a function of V_1/J at ω_1^* is shown in Fig. 3(b). We find that $\langle\chi_1\rangle$ stays close to its initial value at large V_1/J which is consistent with prethermal strong HSF. We have checked that this behavior is similar for all $\langle\chi_j\rangle$.

Next, we study the dynamics of frozen state when $|\psi_f\rangle = |\mathbb{Z}_2\rangle$. As shown in Fig. 3(c), when the system is driven at ω_1^* (blue curve), the equal-time correlation function $\chi_1(nT)$ shows slow oscillations with a time period that is orders of magnitude longer than the bare timescales implied in the Hamiltonian of Eq. (1). On the other hand, the oscillations are absent for $6\omega_1^*$ [red curve in Fig. 3(c)]. In fact, the occurrence of the slow oscillations require two

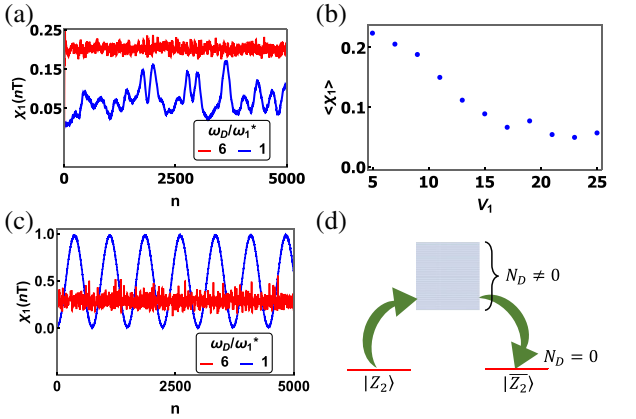

FIG. 3. (a) Plot of $\chi_1(nT)$ as a function of n for $V_1 = 19$ at ω_1^* (blue curve) and $6\omega_1^*$ (red curve) starting from a random frozen state showing lack of ETH predicted thermalization at ω_1^*. (b) Plot of $\langle\chi_1\rangle$ as a function of V_1 at ω_1^*; $\langle\chi_1\rangle$ stays close to its initial value for large V_1 which is consistent with prethermal HSF. (c) Same as in (a) but for initial $|\mathbb{Z}_2\rangle$ state showing slow oscillations at ω_1^*. (d) Schematic diagram for the Floquet quasienergies showing doubly degenerate $|\mathbb{Z}_2\rangle$ and $|\bar{\mathbb{Z}}_2\rangle$ with $N_d = 0$ and other states with $N_d \neq 0$. The arrows indicate transition to $|\bar{\mathbb{Z}}_2\rangle$ from $|\mathbb{Z}_2\rangle$ using intermediate states with $N_d \neq 0$ leading to slow oscillations. For all plots $V_0 = 10V_2 = 2$, $L = 14$, and all energies are scaled in units of J.

conditions to be satisfied. First, the system has to be fragmented in a prethermal sense so that, starting from the state $|\mathbb{Z}_2\rangle$, over long timescales the system stays effectively confined in the $N_D = 0$ sector with no nearest neighbor occupations. This sector comprises the states $|\mathbb{Z}_2\rangle$ and $|\bar{\mathbb{Z}}_2\rangle \equiv |1,0,1,0,\ldots\rangle$. Second, the energy scales $J/V_0 \lesssim 1$ and $V_2/V_0 \leq 1/2$, so that $N_D = 0$ is the lowest energy manifold in the Fock space, while $N_D \neq 0$ are high energy states as shown in Fig. 3(d). In such a situation the higher order terms in FPT provide tunneling paths for the system to oscillate between $|\mathbb{Z}_2\rangle$ and $|\bar{\mathbb{Z}}_2\rangle$. Since $\hat{n}_1\hat{n}_3|\mathbb{Z}_2\rangle = 0$, while $\hat{n}_1\hat{n}_3|\bar{\mathbb{Z}}_2\rangle = 1$, the equal-time correlation function $\chi_1(nT)$ oscillates between zero and nearly one (the deviation from one is due to finite mixing with the states in the $N_D \neq 0$ sectors). In other words, the oscillations are manifestation of the tunneling processes that restore Z_2 symmetry in a finite system such that the approximate eigenstates of H_F are the bonding and antibonding states $|\psi_{B,A}\rangle \equiv |\mathbb{Z}_2\rangle \pm |\bar{\mathbb{Z}}_2\rangle$. Therefore, the oscillation frequency is proportional to the energy split $2\hbar\alpha_d$ between the bonding and antibonding states; this is expected to be a small energy scale as it arises from higher order terms in H_F (which we verified using ED). Thus, if $H_F|\psi_{B,A}\rangle \approx \hbar(\alpha_s \pm \alpha_d)|\psi_{B,A}\rangle$ for a constant α_s, one can show that $\chi_1(nT) \approx \sin^2(\alpha_d nT)$ which explains the slow oscillations. In passing, we note that similar oscillations also appear in the fidelity function $F(nT) \equiv |\langle\mathbb{Z}_2(0)|\mathbb{Z}_2(nT)\rangle|^2$ [41].

Discussion.—In conclusion, we have proposed a novel mechanism to obtain the first realization of prethermal strong HSF in a periodically driven fermionic chain at $\omega_D = \omega_m^*$. We support this claim by exact numerical computation of entanglement entropy, autocorrelation, and equal-time correlation functions of the fermions and provide analytic expression of ω_m^* using FPT. We have also studied the dynamics of these fermions starting from frozen states and have identified a novel oscillatory dynamics for the $|\mathbb{Z}_2\rangle$ initial state; such oscillations arise due to both HSF and Z_2 symmetry breaking. We expect our results to be of relevance for ultracold atom platforms where such fermion chains may be experimentally realized [35,47].

S. G. acknowledges CSIR, India for support through Project No. 09/080(1133)/2019-EMR-I. I. P. thanks Edouard Boulat for discussions. K. S. thanks DST, India for support through SERB Project No. JCB/2021/000030 and Arnab Sen for discussions.

[1] J. M. Deutsch, Phys. Rev. A **43**, 2046 (1991); M. Srednicki, Phys. Rev. E **50**, 888 (1994); J. Phys. A **32**, 1163 (1999).
[2] M. Rigol, V. Dunjko, and M. Olshanii, Nature (London) **452**, 854 (2008); P. Reimann, Phys. Rev. Lett. **101**, 190403 (2008).
[3] A. Polkovnikov, K. Sengupta, A. Silva, A., and M. Vengalattore, Rev. Mod. Phys. **83**, 863 (2011).
[4] L. D'Alessio, Y. Kafri, A. Polkovnikov, and M. Rigol, Adv. Phys. **65**, 239 (2016).
[5] L. D'Alessio and M. Rigol, Phys. Rev. X **4**, 041048 (2014).
[6] M. Bukov, L. D'Alessio, and A. Polkovnikov, Adv. Phys. **64**, 139 (2015).
[7] W. W. Ho, T. Mori, D. A. Abanin, and E. G. Dalla Torre, arXiv:2212.00041.
[8] T. Kohlert, S. Scherg, X. Li, H. P. Luschen, S. Das Sarma, I. Bloch, and M. Aidelsburger, Phys. Rev. Lett. **122**, 170403 (2019).
[9] A. Kyprianidis, F. Machado, W. Morong, P. Becker, K. S. Collins, D. V. Else, L. Feng, P. W. Hess, C. Nayak, G. Pagano, N. Y. Yao, and C. Monroe, Science **372**, 1192 (2021).
[10] A. Das, Phys. Rev. B **82**, 172402 (2010); S. Bhattacharyya, A. Das, and S. Dasgupta, Phys. Rev. B **86**, 054410 (2012); S. S. Hegde, H. Katiyar, T. S. Mahesh, and A. Das, Phys. Rev. B **90**, 174407 (2014).
[11] A. Haldar, R. Moessner, and A. Das, Phys. Rev. B **97**, 245122 (2018); A. Haldar, D. Sen, R. Moessner, and A. Das, Phys. Rev. X **11**, 021008 (2021).
[12] T. Banerjee and K. Sengupta, arXiv:2209.12939.
[13] A. Agarwala, U. Bhattacharya, A. Dutta, and D. Sen, Phys. Rev. B **93**, 174301 (2016); A. Agarwala and D. Sen, Phys. Rev. B **95**, 014305 (2017).
[14] D. J. Luitz, Y. Bar Lev, and A. Lazarides, SciPost Phys. **3**, 029 (2017); D. J. Luitz, A. Lazarides, and Y. Bar Lev, Phys. Rev. B **97**, 020303(R) (2018).
[15] R. Ghosh, B. Mukherjee, and K. Sengupta, Phys. Rev. B **102**, 235114 (2020).
[16] D. V. Else, B. Bauer, and C. Nayak, Phys. Rev. Lett. **117**, 090402 (2016).
[17] B. Mukherjee, S. Nandy, A. Sen, D. Sen, and K. Sengupta, Phys. Rev. B **101**, 245107 (2020).
[18] B. Mukherjee, A. Sen, D. Sen, and K. Sengupta, Phys. Rev. B **102**, 014301 (2020).
[19] M. Basko, I. L. Aleiner, and B. L. Altshuler, Ann. Phys. (Amsterdam) **321**, 1126 (2006).
[20] R. Nandkishore and D. Huse, Annu. Rev. Condens. Matter Phys. **6**, 15 (2015).
[21] C. J. Turner, A. A. Michailidis, D. A. Abanin, M. Serbyn, and Z. Papić, Nat. Phys. **14**, 745 (2018); S. Moudgalya, N. Regnault, and B. A. Bernevig, Phys. Rev. B **98**, 235156 (2018).
[22] W. W. Ho, S. Choi, H. Pitchler, and M. D. Lukin, Phys. Rev. Lett. **122**, 040603 (2019); N. Shiraishi, J. Stat. Mech. (2019) 08313.
[23] S. Choi, C. J. Turner, H. Pichler, W. W. Ho, A. A. Michailidis, Z. Papić, M. Serbyn, M. D. Lukin, and D. A. Abanin, Phys. Rev. Lett. **122**, 220603 (2019); T. Iadecola, M. Schecter, and S. Xu, Phys. Rev. B **100**, 184312 (2019).
[24] P. A. McClarty, M. Haque, A. Sen, and J. Richter, Phys. Rev. B **102**, 224303 (2020); D. Banerjee and A. Sen, Phys. Rev. Lett. **126**, 220601 (2021); S. Biswas, D. Banerjee, and A. Sen, SciPost Phys. **12**, 148 (2022).
[25] A. Chandran, T. Iadecola, V. Khemani, and R. Moessner, arXiv:2206.11528.
[26] S. Sugiura, T. Kuwahara, and K. Saito, Phys. Rev. Res. **3**, L012010 (2021); P-G Rozon, M. J. Gullans, and K. Agarwal, Phys. Rev. B **106**, 184304 (2022).
[27] B. Mukherjee, A. Sen, and K. Sengupta, Phys. Rev. B **106**, 064305 (2022); A. Hudomal, J-Y Desaules, B. Mukherjee, G.-X Su, J. C. Halimeh, and Z. Papic, Phys. Rev. B **106**, 104302 (2022).
[28] H. Zhao, J. Vovrosh, F. Mintert, and J. Knolle, Phys. Rev. Lett. **124**, 160604 (2020); H. Zhao, A. Smith, F. Mintert, and J. Knolle, Phys. Rev. Lett. **127**, 150601 (2021).
[29] V. Khemani, M. Hermele, and R. Nandkishore, Phys. Rev. B **101**, 174204 (2020).
[30] P. Sala, T. Rakovszky, R. Verresen, M. Knap, and F. Pollmann, Phys. Rev. X **10**, 011047 (2020).
[31] T. Rakovszky, P. Sala, R. Verresen, M. Knap, and F. Pollmann, Phys. Rev. B **101**, 125126 (2020).
[32] Z.-C. Yang, F. Liu, A. V. Gorshkov, and T. Iadecola, Phys. Rev. Lett. **124**, 207602 (2020).
[33] G. De Tomasi, D. Hetterich, P. Sala, and F. Pollmann, Phys. Rev. B **100**, 214313 (2019); P. Frey, L. Hackl, and S. Rachel, Phys. Rev. B **106**, L220301 (2022).
[34] S. Moudgalya and O. I. Motrunich, Phys. Rev. X **12**, 011050 (2022); D. T. Stephen, O. Hart, and R. M. Nandkishore, arXiv:2209.03966; D. Hahn, P. A. McClarty, and D. J. Luitz, SciPost Phys. **11**, 074 (2021); N. Regnault and B. A. Bernevig, arXiv:2210.08019; D. D. Vu, K. Huang, X. Li, and S. Das Sarma, Phys. Rev. Lett. **128**, 146601 (2022).
[35] T. Kohlert, S. Scherg, P. Sala, F. Pollmann, B. H. Madhusudhana, I. Bloch, and M. Aidelsburger, arXiv:2106.15586.

[36] B. Mukherjee, D. Banerjee, K. Sengupta, and A. Sen, Phys. Rev. B **104**, 155117 (2021); P. Brighi, M. Ljubotina, and M. Serbyn, arXiv:2210.15607.
[37] J Lehmann, P Sala, F Pollmann, and T Rakovszky, arXiv: 2208.12260.
[38] A. Chattopadhyay, B. Mukherjee, K. Sengupta, and A. Sen, arXiv:2208.13800.
[39] D. N. Page, Phys. Rev. Lett. **71**, 1291 (1993); L. Vidmar and M. Rigol, Phys. Rev. Lett. **119**, 220603 (2017).
[40] P. Mazur, Physica **43**, 533 (1969); J. Sirker, SciPost Phys. Lect. Notes **17**, 1 (2020).
[41] See Supplemental Material at http://link.aps.org/supplemental/10.1103/PhysRevLett.130.120401 for details.
[42] A. Sen, D. Sen, and K. Sengupta, J. Phys. Condens. Matter **33**, 443003 (2021).
[43] A. Soori and D. Sen, Phys. Rev. B **82**, 115432 (2010).
[44] T. Bilitewski and N. R. Cooper, Phys. Rev. A **91**, 063611 (2015).
[45] T. Mori, T. Kuwahara, and K. Saito, Phys. Rev. Lett. **116**, 120401 (2016); T. Kuwahara, T. Mori, and K. Saito, Ann. Phys. (Amsterdam) **367**, 96 (2016).
[46] S. Vajna, K. Klobas, T. Prosen, and A. Polkovnikov, Phys. Rev. Lett. **120**, 200607 (2018).
[47] I. Bloch, J. Dalibard, and W. Zwerger, Rev. Mod. Phys. **80**, 885 (2008).